Transactions of the Materials Research Society of Japan 28 [3] 711-714 (2003)

Determination of Damaged Region in Composite Structures by Anti-resonant Frequency

Yoshinobu Shimamura, Yoshifumi Okajima*, Akira Todoroki and Hideo Kobayashi
Tokyo Institute of Technology, 2-12-1 O-okayama, Meguro, Tokyo 152-8552, Japan
Fax: 81-3-5734-2809, e-mail: yshimamu@ginza.mes.titech.ac.jp
*Graduate student of Tokyo Institute of Technology

Recently, composite laminated structures have been applied to many structures of vehicles. Since interlaminar strength of composite laminated structures is relatively low, internal damage can be easily induced in service. In order to assess the integrity of the damaged structures, it is necessary to identify the size and position of the damage nondestructively. Natural frequency is often used to identify them. Though natural frequency is easy to measure, application to symmetrical structures is difficult because of symmetry of natural frequency change with respect to the position of damage. The present study proposes a determination technique of the damaged region of smart composite structures with piezoelectric patches using anti-resonance frequency. The change of anti-resonant frequency due to damage is derived mathematically, and the asymmetrical nature of anti-resonant frequency change is verified. Furthermore, determination of a damaged region for a double-end clamped beam is carried out, and it is shown that the technique is useful to determine the damaged region.
Key word: Smart composite structures, Damage identification, Anti-resonant frequency

1. INTRODUCTION

Recently, composite laminated structures have been applied to many structures of vehicles. Since interlaminar strength of composite laminated structures is relatively low, internal damage can be easily induced in service. In order to assess the integrity of the damaged structures, it is necessary to identify the damage nondestructively. Since natural frequency decreases due to damage and is easy to measure, natural frequency change is often used to identify damage [1-5]. However, natural frequency change of structures that have a symmetrical shape and symmetrical boundary conditions has symmetry with respect to the position of damage. That means damage identification of the symmetrical structures by the natural frequency change always has plural candidates of the position of damage.

Inada et al. [6] showed for several composite beams that anti-resonant frequency change is useful to winnow the candidates down, but generality has not been proven yet. Though Inada et al. used an impact hammer method to measure the frequency response, a smart structure system that mounts piezoelectric patches is desirable from the standpoint of health monitoring.

In this study, the frequency response of a smart composite beam that has a PZT actuator and a PVDF sensor is derived, and anti-resonant frequency change is investigated. Based on the result, a determination technique of the region with a damaged segment is proposed. Furthermore, the method is applied to a double-end clamped beam to demonstrate the feasibility of the method. As a result, it is shown that anti-resonant frequency change is useful to determine the region with the damaged segment.

2. ANTI-RESONANT FREQUENCY CHANGE

Although natural frequency change due to damage in composite laminates have been widely studied, little is known about anti-resonant frequency change due to damage in the composite laminates. Advantages of use of anti-resonant frequency for the smart composite structures are that no additional sensor and actuator is required to measure it, and that the change of anti-resonant frequency depends on the positions of the actuator and the sensor. Disadvantage of anti-resonant frequency is difficulty of accurate measurement. Taking account of them, anti-resonant frequency is suitable to an assistant parameter.

For simple mass-spring models, anti-resonant frequency change due to damage, i.e. softening of spring, is easily derived [6]. Let us consider a 3 DOF mass-spring model as shown in Fig.1, for example. As an intact condition, spring constants $k_1=k_2=k_3=k_4=k$ and mass $m_1=m_2=m_3=m$. Mass m_1 is actuated and displacement of mass m_2 is measured. Natural frequency change and anti-resonant frequency change due to damage of the spring k_2 or k_3 is calculated. Damage is modeled as softening of spring $k'=0.8k$.

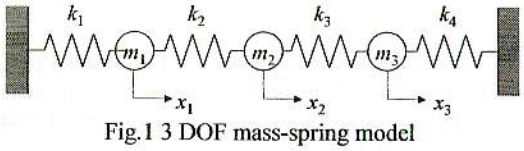

Fig.1 3 DOF mass-spring model

The results are shown in Table I. The results show that the changes of natural frequency due to damage are same for each damaged case but the anti-resonant frequency changes are different. In addition, the anti-resonant frequency does not change in case that k_2 is damaged, whereas the anti-resonant frequency decreases in case that k_3 is damaged. This asymmetrical

nature is useful to determine the region with damage.

Table I Natural frequency and anti-resonant frequency

Position of damage	Natural frequency	Anti-resonant frequency
None	1st: $0.765(k/m)^{0.5}$ 2nd: $1.41(k/m)^{0.5}$ 3rd: $1.85(k/m)^{0.5}$	$(2k/m)^{0.5}$
k_2	1st: $0.759(k/m)^{0.5}$ 2nd: $1.37(k/m)^{0.5}$ 3rd: $1.77(k/m)^{0.5}$	$(2k/m)^{0.5}$
k_3	1st: $0.759(k/m)^{0.5}$ 2nd: $1.37(k/m)^{0.5}$ 3rd: $1.77(k/m)^{0.5}$	$(1.8k/m)^{0.5}$

In the following sections, anti-resonant frequency change of a smart composite beam with damage is investigated.

2. FREQUENCY RESPONSE

2.1 Model

In order to demonstrate the feasibility of the proposed technique, an Euler-Bernoulli beam model is adopted. For simplicity, it is assumed that beam is homogeneous and damage is modeled as bending stiffness degradation. The configuration of the beam is shown in Fig.1. The beam is divided into three spanwise segments, and there is a damaged segment between two intact segments.

A couple of PZT patches are mounted to accelerate the beam, and a PVDF patch is mounted to measure the vibration.

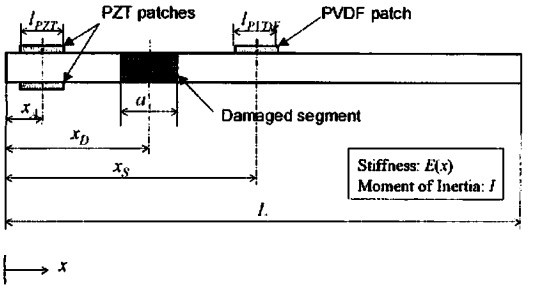

Fig.2 Model configuration

2.3 Frequency response function

The dynamic equation of motion with external force $F(x,t)$ is

$$\rho A\frac{\partial^2 w}{\partial t^2}+\frac{\partial^2}{\partial x^2}(EI\frac{\partial^2 w}{\partial x^2})=F(x,t) \tag{1}$$

where ρ is density, A is the area of the cross section, EI is the bending stiffness and w is the lateral displacement. The displacement w is expressed by using a natural modal function $W_i(x)$ as

$$w=\sum_{i=1}^{\infty}W_i(x)\xi_i(t) \tag{2}$$

Derivation of the natural modal function of the damaged beam is described in Ref. [7]. Substituting eqn. (2) to eqn. (1) gives

$$\rho A\sum_{i=1}^{\infty}W_i\frac{d^2\xi_i}{dt^2}+\sum_{i=1}^{\infty}\frac{d^2}{dx^2}\left(EI\frac{d^2W_i}{dx^2}\right)\xi_i=F(x,t) \tag{3}$$

The dynamic equation of motion for free vibration is

$$\rho A\frac{\partial^2 w}{\partial t^2}+\frac{\partial^2}{\partial x^2}(EI\frac{\partial^2 w}{\partial x^2})=0 \tag{4}$$

We may assume $w=W_i e^{j\omega t}$. Eqn. (4) becomes

$$\frac{d^2}{dx^2}\left(EI\frac{d^2W_i}{dx^2}\right)=\rho A\omega_i^2 W_i \tag{5}$$

Substituting eqn. (5) to eqn. (3) gives

$$\sum_{i=1}^{\infty}W_i(\ddot{\xi}_i+\omega_i^2\xi_i)=\frac{F(x,t)}{\rho A} \tag{6}$$

After multiplying both sides by W_j, integrating the both sides from 0 to L gives

$$\ddot{\xi}_j+\omega_j^2\xi_j=q_j(t) \tag{7}$$

where

$$q_j(t)=\frac{1}{\rho A\kappa_j}\int_0^l F(x,t)W_j(x)dx \tag{8}$$
$$\kappa_j=\int_0^l W_j(x)W_j(x)dx$$

by considering orthogonality.

The actuation force by the PZT sensors is described as follows [8].

$$F(x,t)=M_{eq}f(x)e^{j\omega t} \tag{9}$$

where M_{eq} is the equivalent moment induced by the PZT patches, and $f(x)$ is the function of the positions of concentrated moments induced by the PZT patches.

$$M_{eq}=\frac{C_0 d_{31}V_{PZT}}{t_{PZT}},C_0=\frac{t^2E}{6+\Psi}b_{PZT},\Psi=\frac{tE}{t_{PZT}E_{PZT}} \tag{10}$$

where d_{31} is the piezoelectric dielectric strain constant, V_{PZT} is the applied voltage amplitude, t_{PZT} is the thickness of the PZT patches, E_{PZT} is Young's modulus of the PZT patches. $f(x)$ depends on the position of the PZT actuator and the damaged segment. $f(x)$ in case that the damaged segment is not underneath the PZT actuator is

$$f(x)=\delta'\left(x-\left(x_A-l_2/2\right)\right)-\delta'\left(x-\left(x_A+l_2/2\right)\right) \tag{11}$$

where $\delta'(x)$ is the first derivative of Dirac delta function. $f(x)$ in case that damaged segment is underneath PZT actuators can be similarly expressed.

Eqn. (8) can be written

$$q_j(t) = \frac{1}{\rho A \kappa_j} \int_0^L M_{eq} f(x) e^{j\omega t} W_j(x) dx \tag{10}$$

Eqn. (7) in the case that the damaged segment is not underneath the PZT actuator becomes

$$\xi_j = \frac{M_{eq}}{\rho A \kappa_j} \frac{\left(W_j'\left(x_A + l_{PZT}/2\right) - W_j'\left(x_A - l_{PZT}/2\right)\right)}{(\omega_j^2 - \omega^2)} \tag{11}$$

For other cases, similar derivations hold.

Substituting eqn. (11) to (2), displacement w becomes

$$w = \sum_{i=1}^{\infty} W_i(x) \frac{M_{eq}}{\rho A \kappa_i} \frac{\left(W_i'\left(x_A + l_{PZT}/2\right) - W_i'\left(x_A - l_{PZT}/2\right)\right)}{(\omega_i^2 - \omega^2)} e^{j\omega t} \tag{12}$$

The PVDF output ϕ is described as follows [9].

$$\phi = \frac{e_{31}}{\varepsilon_{31}} \cdot \frac{t_{PVDF}(t + t_{PVDF})}{2} \int_{x_s - l_{PVDF}/2}^{x_s + l_{PVDF}/2} \frac{\partial^2 w}{\partial x^2} dx \tag{13}$$

$$= \frac{e_{31}}{\varepsilon_{31}} \cdot \frac{t_{PVDF}(t + t_{PVDF})}{2} \left(\left.\frac{\partial w}{\partial x}\right|_{x_s + l_{PVDF}/2} - \left.\frac{\partial w}{\partial x}\right|_{x_s - l_{PVDF}/2} \right)$$

where e_{31} is the piezoelectric constant and ε_{31} is the dielectric constant. Therefore, Frequency response function $G(\omega)$ is described as

$$G(\omega) = \frac{\phi}{V_{PZT}} = \frac{e_{31}}{\varepsilon_{31}} \cdot \frac{t_{PVDF}(t + t_{PVDF})}{2} \cdot \frac{C_0 d_{31}}{t_{PZT}} \cdot \sum_{i=1}^{\infty} \frac{1}{\rho A \kappa_i} \frac{\left(W_i'\left(x_A + \frac{l_{PZT}}{2}\right) - W_i'\left(x_A - \frac{l_{PZT}}{2}\right)\right)\left(W_i'\left(x_s + \frac{l_{PVDF}}{2}\right) - W_i'\left(x_s - \frac{l_{PVDF}}{2}\right)\right)}{(\omega_i^2 - \omega^2)} \tag{14}$$

4. RESULTS AND DISCUSSION

The changes of natural and anti-resonant frequencies of a double-end clamped beam are numerically investigated as an example of symmetrical structures.

4.1 Natural frequency

The beam has 200 mm length, 19 mm width and 1.45 mm thickness. Longitudinal Young's modulus is 114GPa and density is 1466 kg/m^3. Damaged segment length a/L is 0.025, 0.05, 0.075 or 0.01. Stiffness is degraded at the damaged segment, and degradation ratio E'/E is 0.95, 0.9, 0.85 or 0.8.

Fig. 3 shows the changes of the first five natural frequencies of the damaged beam (a/L=0.1, E'/E=0.8). Vertical axis is ith eigenvalue λ_i normalized by λ_0, which is λ of an intact beam, and horizontal axis is the position of the damaged segment. In cases of other damaged segment length and/or stiffness degradation ratio, the shapes of the natural frequency changes are similar, and the amplitudes are almost proportionate to the damaged segment length and the stiffness degradation ratio.

The changes of natural frequencies are symmetrical with respect to the center of the beam because the beam shape and boundary conditions are symmetrical with respect to the center of the beam. That means any damage identification methods using the natural frequency change indicates two candidates of the position of the damaged segment.

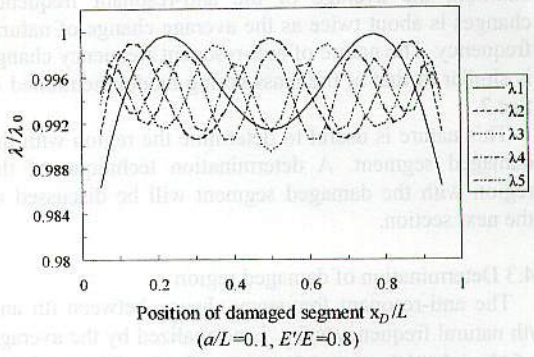

Fig.3 Natural frequency changes due to damage

4.2 Anti-resonant frequency

In order to determine the half of the beam where the damaged segment exists, an actuator of PZT patches is mounted at 0.05L, and a PVDF sensor is mounted at 0.45L. 0.5L is not suitable because several nodes of modal shapes exist at 0.5L. The sensor and actuator lengths are set to 0.1 L. Anti-resonant frequencies can be numerically calculated from eqn. (14).

Fig. 4 shows the change of the first two anti-resonant frequencies (a/L=0.1, E'/E=0.8). Vertical axis is anti-resonant frequency between ith and jth natural frequency $\lambda_{ij}' = (\omega_{ij}^2 \rho A/EI)^{1/4}$ normalized by λ'_0, which is λ' of an intact beam, and horizontal axis is the position of the damaged segment. The anti-resonant frequencies are obviously asymmetrical with respect to the center of the beam. In cases of other damaged segment length and/or stiffness degradation ratio, the shapes of the anti-resonant frequency change are similar, and the amplitudes are almost proportionate to the damaged segment length and the stiffness degradation ratio.

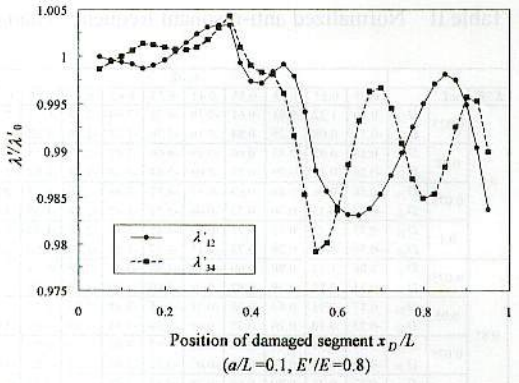

Fig.4 Anti-resonant frequency change due to damage

Eqn. (14) includes natural modal functions, which are asymmetrical if a damaged segment exists in the either half of the beam. Thus the anti-resonant frequency changes are always asymmetrical. The degree of asymmetry depends on the geometrical shape and boundary conditions.

For the double-end clamped beam, the anti-resonant frequency considerably decreases if damage exists beyond the sensor position, whereas the change of anti-resonant frequency is small if damage exists

between the actuator position and the sensor position. In addition, the average of the anti-resonant frequency changes is about twice as the average change of natural frequency. The nature of anti-resonant frequency change is similar to that of the mass-spring model mentioned in Sec.2.

This nature is useful to determine the region with the damaged segment. A determination technique of the region with the damaged segment will be discussed in the next section.

4.3 Determination of damaged region

The anti-resonant frequency change between ith and jth natural frequency $\Delta f_{A,ij}$ is normalized by the average of ith and i+1th natural frequency change $\Delta f_{R,i}$ and $\Delta f_{R,i+1}$ in order to eliminate the influence of damage length and stiffness degradation ratio.

$$D_{ij} = \frac{2\Delta f_{A,ij}}{|\Delta f_{R,i}| + |\Delta f_{R,i+1}|} \tag{15}$$

In case of $0<x_D/L<0.5$, all of normalized anti-resonant frequency changes D_{ij} should be almost 0. In case of $0.5< x_D/L<1$, either of D_{ij}s should significantly decrease. D_{ij}s of 160 cases were calculated; stiffness degradation ratio E'/E is 0.95, 0.9, 0.85 or 0.8, damaged segment length a/L is 0.025, 0.05, 0.075 o 0.1, and the position of the damaged segment x_D/L is 0.15, 0.25, ... 0.95. Table II shows the first two normalized anti-resonant frequency changes D_{23} and D_{45}. D_{12} and D_{34} do not appear in these cases.

In order to determine a threshold of D_{ij}, statistical analysis was carried out for D_{ij} values. For $0<x_D/L<0.5$, the average of D_{ij} is 0.30 and the standard deviation is 0.42. For $0.5<x_D/L<1$, the average of D_{ij} is –2.41 and the standard deviation is 1.1. The threshold value D_{th} is set to –1 by taking into account 3σ of D_{ij}s for $0<x_D/L<0.5$. D_{th} is about half of the average in case of $0.5<x_D/L<1$. White cells in table I represent $D_{ij}>D_{th}$, and gray cells represent $D_{ij}<D_{th}$.

Table II Normalized anti-resonant frequency change

E'/E	a/L		x_D/L 0.05	0.15	0.25	0.35	0.45	0.55	0.65	0.75	0.85	0.95
0.8	0.025	D_{23}	0.06	1.22	0.81	0.61	-0.18	-4.70	-3.49	-2.58	-0.27	-2.21
		D_{45}	-0.11	0.08	0.29	0.84	0.10	-3.70	-1.28	-1.88	-1.88	-1.83
	0.05	D_{23}	0.18	0.93	0.85	0.66	-0.19	-4.66	-3.47	-2.57	-0.53	-2.21
		D_{45}	-0.26	0.10	0.29	0.73	0.04	-3.64	-1.38	-1.87	-1.88	-1.82
	0.075	D_{23}	0.36	0.56	0.88	0.69	-0.22	-4.57	-3.48	-2.58	-0.87	-2.20
		D_{45}	-0.45	0.13	0.30	0.73	-0.04	-3.53	-1.45	-1.84	-1.89	-1.82
	0.1	D_{23}	0.55	0.23	0.92	0.71	-0.27	-4.45	-3.49	-2.58	-1.19	-2.19
		D_{45}	-0.59	0.18	0.28	0.73	-0.15	-3.37	-1.55	-1.80	-1.90	-1.82
0.85	0.025	D_{23}	0.06	1.14	0.80	0.60	-0.19	-4.69	-3.49	-2.58	-0.33	-2.22
		D_{45}	-0.11	0.11	0.28	0.82	0.09	-3.69	-1.29	-1.88	-1.88	-1.83
	0.05	D_{23}	0.17	0.91	0.83	0.63	-0.21	-4.65	-3.48	-2.58	-0.53	-2.21
		D_{45}	-0.25	0.10	0.28	0.75	0.05	-3.64	-1.36	-1.86	-1.89	-1.82
	0.075	D_{23}	0.34	0.54	0.86	0.66	-0.23	-4.55	-3.49	-2.59	-0.86	-2.21
		D_{45}	-0.42	0.13	0.28	0.73	-0.05	-3.52	-1.46	-1.84	-1.89	-1.82
	0.1	D_{23}	0.53	0.21	0.89	0.68	-0.28	-4.43	-3.49	-2.60	-1.18	-2.20
		D_{45}	-0.57	0.18	0.28	0.72	-0.15	-3.36	-1.56	-1.80	-1.90	-1.82
0.9	0.025	D_{23}	0.06	1.15	0.79	0.59	-0.19	-4.68	-3.49	-2.59	-0.31	-2.22
		D_{45}	-0.11	0.10	0.28	0.81	0.08	-3.69	-1.29	-1.87	-1.89	-1.83
	0.05	D_{23}	0.17	0.82	0.81	0.61	-0.21	-4.63	-3.49	-2.59	-0.60	-2.22
		D_{45}	-0.25	0.13	0.27	0.80	0.04	-3.63	-1.36	-1.86	-1.89	-1.83
	0.075	D_{23}	0.33	0.52	0.83	0.63	-0.25	-4.54	-3.49	-2.60	-0.86	-2.22
		D_{45}	-0.41	0.14	0.26	0.73	-0.03	-3.52	-1.46	-1.84	-1.89	-1.82
	0.1	D_{23}	0.52	0.20	0.85	0.64	-0.30	-4.40	-3.49	-2.62	-1.18	-2.21
		D_{45}	-0.56	0.18	0.26	0.72	-0.16	-3.35	-1.57	-1.80	-1.90	-1.82
0.95	0.025	D_{23}	0.05	1.15	0.78	0.60	-0.19	-4.67	-3.47	-2.59	-0.30	-2.22
		D_{45}	-0.11	0.09	0.27	0.75	0.08	-3.68	-1.35	-1.87	-1.89	-1.83
	0.05	D_{23}	0.16	0.84	0.79	0.60	-0.22	-4.62	-3.48	-2.60	-0.57	-2.22
		D_{45}	-0.26	0.12	0.26	0.75	0.03	-3.61	-1.39	-1.86	-1.89	-1.83
	0.075	D_{23}	0.32	0.47	0.81	0.60	-0.26	-4.52	-3.50	-2.62	-0.89	-2.22
		D_{45}	-0.41	0.16	0.25	0.76	-0.05	-3.50	-1.46	-1.84	-1.90	-1.82
	0.1	D_{23}	0.50	0.15	0.83	0.60	-0.31	-4.39	-3.50	-2.63	-1.21	-2.23
		D_{45}	-0.53	0.21	0.24	0.76	-0.15	-3.35	-1.57	-1.80	-1.91	-1.82

All of D_{ij}s satisfy $D_{ij} > D_{th}$ in case of $0.5<x_D/L<1$. Either of D_{ij}s is $D_{ij} < D_{th}$ in case of $0<x_D/L<0.5$. In other words, the region with the damaged segment can be accurately determined by the method.

Since the asymmetrical nature of anti-resonant frequency change holds for any symmetric structures, we can apply the proposed method to any symmetrical composite structures.

5. CONCLUSIONS

Determination of a damaged region in symmetrical smart composite structures by anti-resonant frequency is proposed. The change due to damage is derived mathematically, and the asymmetrical nature of anti-resonant frequency is proved. Furthermore, determination of the damaged region in a double-end clamped beam is demonstrated.

6.REFERENCES

[1] A.S.Islam and K.C.Craig, Smart Mater. Struct, 3, 3, 318-328 (1994)

[2] A.C.Okafor, K.Chandrashekhara and Y.P.Jiang, Smart Mater. Struct. 5, 3, 338-347(1996)

[3] O.Byon and Y.Nishi, Key Engineering Matcrials, 141-143, 1, 55-64(1998)

[4] T.Inada, Y.Shimamura, A.Todoroki, H.Kobayashi and H.Nakamura, Tras.Jpn.Soc.Mech.Eng., 65, 632A, 776-782(1999) (in Japanese)

[5] S.E.Watkins, G.W.Sanders, F.Akhavan and K.Chandrashekhara, Smart Mater. Struct., 11, 489-495(2002)

[6] T.Inada, Y.Shimamura, A.Todoroki and H.Kobayashi, Tras.Jpn.Soc.Mech.Eng., 67, 664A, 1929-1935(2001) (in Japanese)

[7] Y.Shimamura, H.S.Tzou, A.Todoroki and H.Kobayashi, Mech.Sys.Sig.Proc., (under submitting)

[8] B.S.Wang and C.C.Wang, Smart Mater. Struct., 6, 106-116(1997)

[9] R.V.Howard, W.K.Chai and H.S.Tzou, Mech.Sys.Sig.Proc., 15, 3, 629-640(2001)

(Received December 21, 2002; Accepted Febuary 14, 2003)